Journal of Applied Physics

Bound photoinduced giant spin polaron in EuTe

Cite as: J. Appl. Phys. **131**, 043903 (2022); https://doi.org/10.1063/5.0079384
Submitted: 20 November 2021 • Accepted: 04 January 2022 • Published Online: 25 January 2022

A. B. Henriques, S. C. P. van Kooten, E. Abramof, et al.

View Online Export Citation CrossMark

AIP Publishing

Applied Physics Reviews

Read. Cite. Publish. Repeat.

19.162
2020 IMPACT FACTOR*

AIP Publishing

© 2022 Author(s).

Journal of Applied Physics ARTICLE scitation.org/journal/jap

Bound photoinduced giant spin polaron in EuTe

Cite as: J. Appl. Phys. **131**, 043903 (2022); doi: 10.1063/5.0079384
Submitted: 20 November 2021 · Accepted: 4 January 2022 ·
Published Online: 25 January 2022

View Online Export Citation CrossMark

A. B. Henriques,[1,a)] S. C. P. van Kooten,[1] E. Abramof,[2] P. H. O. Rappl,[2] and G. D. Galgano[1]

AFFILIATIONS

[1]Instituto de Fisica, Universidade de Sao Paulo, 05508-090 Sao Paulo, Brazil
[2]LAS-INPE, Av. dos Astronautas, 1758—Jd. Granja, 12227-010 São José dos Campos, Brazil

[a)]**Author to whom correspondence should be addressed:** andreh@if.usp.br

ABSTRACT

Previously, we showed that at low temperatures and very low excitation powers, EuTe displays band-edge photoluminescence with a well-resolved phonon structure, the so-called MX_0 band, which is associated with the recombination of giant spin polarons (SPs) of magnetic moments of several hundred Bohr magnetons. Here, we investigate the MX_0 band both experimentally and by Monte Carlo simulations. Results indicate that the SPs are bound to defects, with a localization energy of 0.29 eV. The density of defects harboring the SPs is estimated to be 4.3×10^{15} cm^{-3}.

Published under an exclusive license by AIP Publishing. https://doi.org/10.1063/5.0079384

I. INTRODUCTION

Many decades ago, de Gennes predicted that in magnetic semiconductors, charge carriers could self-trap by altering the alignment of localized spins in its surroundings,[1] forming a magnetic polaron or a spin polaron (SP).[2,3] Subsequent theoretical studies indicated that, in intrinsic magnetic semiconductors, such as europium chalcogenides, a SP could not be formed by a free conduction band electron alone because the latter did not have the power to polarize its surroundings enough to create a bound state. However, if the electron was bound to a hole forming an exciton, then an SP would be formed[4,5] (see also Ref. 6 for a self-consistent treatment of the SP).

The theoretical predictions motivated experiments to detect SPs. While SPs were largely reported in diluted magnetic semiconductors,[7] their detection in intrinsic magnetic semiconductors proved to be much more difficult. In 2009, von Molnar and collaborators[8] described the detection of SPs in intrinsic magnetic semiconductors a "formidable challenge" and reported the first direct observation of SPs in EuS, whose magnetic moment was found to be 36 Bohr magnetons (μ_B), at 90 K when EuS is in the paramagnetic phase.

More recently, from photoluminescence (PL) measurements, the magnetic moment of the photoexcited SPs in EuTe was found to be giant by comparison, reaching almost $700\,\mu_B$.[6,9] The much larger than ever previously reported SP was detected at a lower temperature ($T = 5$ K), where the magnetic susceptibility of the lattice is high. The size of the SP was confirmed by steady-state photoinduced Faraday rotation measurements.[10] Subsequently, supergiant ($7000\,\mu_B$) and hypergiant ($20\,000\,\mu_B$) photoexcited SPs were found in EuSe[11] and EuS,[12] respectively. The radius and spin texture of the SPs were also determined, as well as the temperature and magnetic field dependencies of the SP parameters.[10,13] The dynamics of SP generation was also investigated, and it was found that SPs can be generated on the ultrafast time scale.[11] These discoveries pave the way for ultrafast magneto-optical applications, using the optical control of the magnetic state of europium chalcogenides.

Despite all the progress, a fundamental question is still open, is the electronic state that hosts photoinduced SPs in europium chalcogenides intrinsic or associated with imperfections? This information is crucial to achieve efficient light manipulation of the magnetization in europium chalcogenides.

In this work, we focus on EuTe. Based on a combination of PL experiments and Monte Carlo simulations, we show that the giant SPs detected in EuTe are bound to defects. The localization energy of the SP is estimated to be 0.29 eV, and the defect density is found to be 4.3×10^{15} cm^{-3}.

II. EXPERIMENTAL

The EuTe samples were grown at LAS-INPE by molecular beam epitaxy (MBE) on a (111)-oriented BaF_2 substrate, as described in Ref. 14.

For the PL measurements, the excitation source was a Nd:YAG 532 nm laser. Light was conveyed to the sample and collected

Published under an exclusive license by AIP Publishing

from the sample, using optical fibers, which is essential to gather efficiently the small amount of light the sample produces under the very low excitation levels employed here. More details of the PL experiment are given in Ref. 15.

All samples were grown from high purity precursors and were nominally undoped. We measured the PL of three samples, with EuTe epitaxial layers of thickness 1.0, 1.5, and 4.2 μm, respectively. When the excitation laser power density was below 1 mW/cm^2, all samples showed the same phonon replicas, with PL intensities described by a Poisson distribution.[9] The temperature and excitation power dependencies of the PL were also the same for all samples. More detailed measurements were performed for the sample with an epilayer thickness of 1.0 μm whose PL was least affected by the Fabry–Perot interference in the epilayer,[9] and the results are presented here.

III. THE MX_0 PL BAND AT 4.8 K

Figure 1(a) shows the EuTe band-edge PL at 4.8 K, measured at a very low excitation power (0.1 mW/cm^2), showing the MX_0 band.

The MX_0 luminescence, as well as other band-edge magneto-optical properties of europium chalcogenides, can be described by an atomic valence level $4f^7(^8S_{7/2})$, strongly localized at an Eu atom, and a $5d(t_{2g})$ conduction band, built from Eu 5d states, split in the crystal field.[16] These electronic states are sufficient to describe theoretically very well the linear[17–20] and non-linear[21–23] band-edge optical properties of europium chalcogenides.

The MX_0 band is due to the recombination of giant SPs, formed by an electron bound to a hole in the $4f^7(^8S_{7/2})$ state, surrounded by a halo of canted lattice spins.[6,9] The SP recombination is coupled to LO-phonons, of energy 18 meV,[24] showing several phonon replicas. For a better resolution of the phonon replicas, the second derivative of the PL spectrum was taken. To reduce the noise, prior to taking the second derivative, the PL spectra were low pass filtered, through a convolution with a Gaussian of full width at half maximum (FWHM) of about 10 meV. The second derivative obtained this way is plotted in Fig. 1(b): phonon emissions $N = 0, 1, \ldots, 5$ can be clearly resolved. The pure SP recombination, with $N = 0$ phonon emission—the zero phonon line (ZPL)[25]—is indicated by the arrow.

To describe the energy of the ZPL, we shall exploit the well-established knowledge of excitonic recombination in semiconductors.[26–28] An SP is just an exciton, surrounded by a halo of canted lattice spins. Excitons can be either free or bound to defects or impurities. If no phonons are emitted, the photon energy produced in the exciton recombination is given by the energy required to form the exciton for which the general expression, in the effective mass approximation, is given by[26]

$$h\nu_{\mathrm{EXCITON}} = E_G - R^* - E_{\mathrm{loc}}, \tag{1}$$

where E_G is the bandgap, R^* is the effective Rydberg (i.e., the free exciton binding energy), and E_{loc} is the localization energy of the exciton (for a free exciton, $E_{\mathrm{loc}} = 0$).

For an SP, the recombination energy is further reduced by the self-energy, Σ, which the electron loses by inducing spin polarization in the surroundings. The SP recombination ZPL photon energy is then given by

$$h\nu_{\mathrm{ZPL}} = E_G - R^* - \Sigma - E_{\mathrm{loc}}. \tag{2}$$

We shall determine E_{loc} by measuring the temperature dependence of the ZPL photon energy and fitting the result with Monte Carlo simulations (MCS), whereby E_{loc} is the sole adjustable parameter.

Figure 2 shows a stack plot of the second derivative of the MX_0 band, measured in the 4.8–20 K interval. Above 20 K, the MX_0 PL intensity becomes too weak to be measured with sufficient precision. The MX_0 band shows a large blueshift when temperature increases. The MX_0 blueshift is due to increasing thermal agitation of spins, which reduces the lattice magnetic susceptibility and

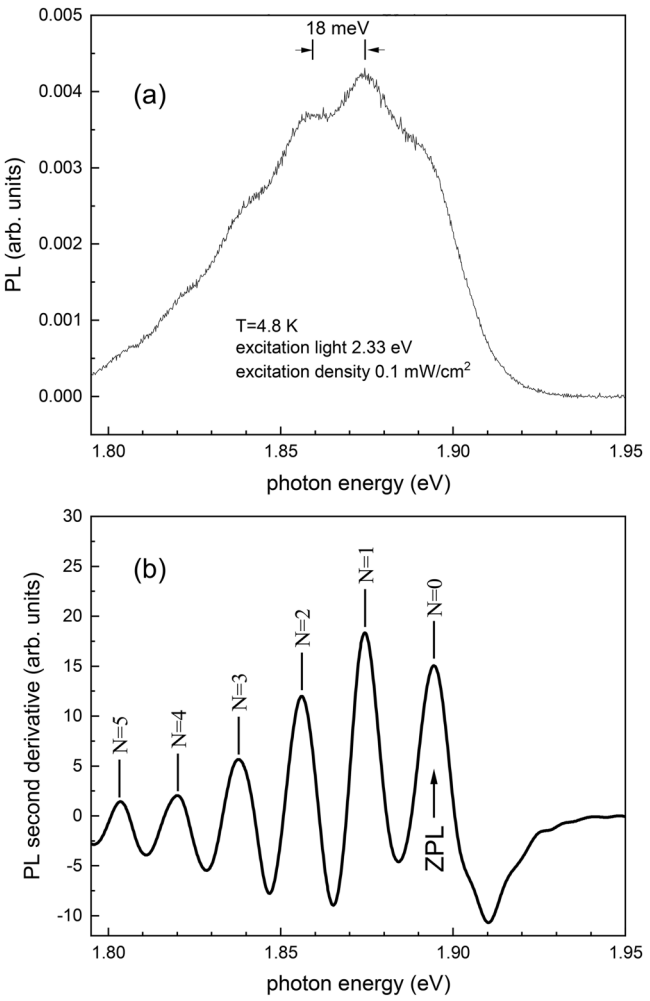

FIG. 1. (a) PL spectrum of the EuTe sample at 4.8 K, using a photon energy of 2.33 eV and a very low excitation density of 0.1 mW/cm^2. (b) Negative of the second derivative of the PL spectrum. The pure electronic transition with zero phonons emitted—the ZPL line—is indicated.

Published under an exclusive license by AIP Publishing

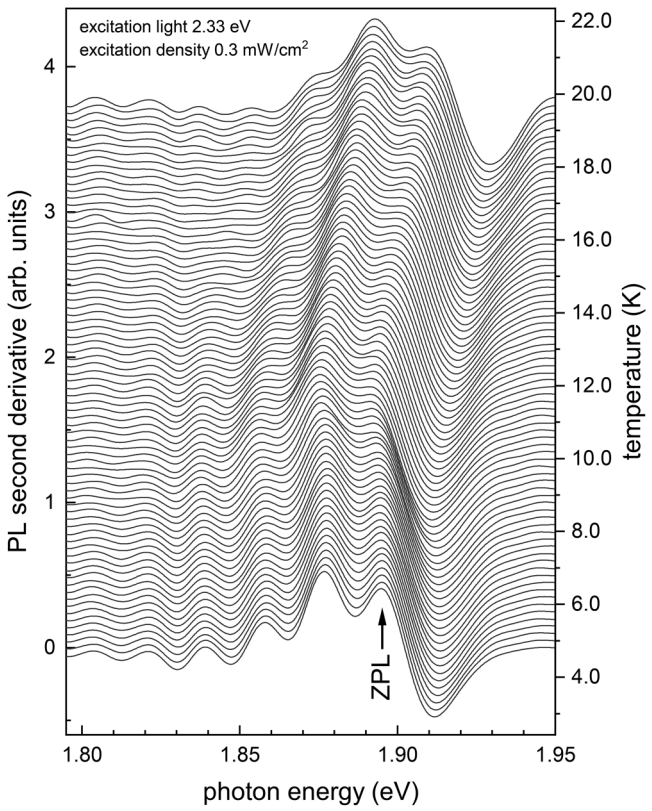

FIG. 2. Stacked plot of the negative of the second derivative of the PL spectra as a function of temperature, taken with an excitation power of 0.35 mW/cm^{-2}. The temperature corresponding to each curve is obtained by following the spectrum baseline to the scale on the right-hand side.

hence the self-energy, Σ, of the photoexcited electron. In general, by destroying the lattice spin polarization, a temperature increase will make the SP self-consistent potential less binding,[6] which causes the Bohr radius to increase; thus, it will also reduce R^*. However, the main binding force for the SP in europium chalcogenides comes from the Coulomb attraction to the hole. This is even more pronounced in EuTe, where the SP is of type-I;[9] i.e., a ferromagnetic core is absent due to the antiferromagnetic resistance to spin alignment. This implies that the self-consistent potential is not hugely dependent on spin polarization within the SP, hence to a good approximation, the effective Bohr radius and R^* are temperature independent,[6] especially in the low temperature interval examined in this work.

We describe here very briefly the MCS procedure; a detailed description is given in Ref. 13. Eu spins were distributed in the EuTe fcc lattice of parameter a. A cube, whose edge was equal to 8 a, was singled out. Periodic Born-von Kármán boundary conditions were imposed on the Eu spins in the cube. To simulate a SP, a photoexcited electron was placed in the center of the cube. The SP is formed due to the effective exchange magnetic field, B_{Xf}, that the photoexcited electron imposes on the lattice spins, which at a distance r from the photoexcited electron is given by[6]

$$B_{Xf}(r) = \frac{J_{Xf}S}{N\mu^*}\Psi^2(r), \tag{3}$$

where J_{Xf} is the electron–lattice exchange interaction constant, N and S are the volume density and magnetic quantum number of lattice spins, respectively, $\mu^* = g_S\mu_B S$ is the magnetic moment of an Eu atom, g_S is the Landé factor, μ_B is the Bohr magneton, $\Psi(r) = \frac{e^{-r/a_B}}{\sqrt{\pi a_B{}^3}}$ is the Bohr wavefunction of the photoexcited electron, and a_B is the effective Bohr radius. For EuTe, $g_S = 2$, $S = 7/2$, $N = 4/a^3$, $a = 6.6$ Å, and $a_B = 1.76\,a$ (this is the self-consistent effective Bohr radius in zero magnetic field, as described in Ref. 6). Since the effective mass of the band-edge electrons in EuTe is $m^* = 0.3\,m_0$,[29] where m_0 is the free electron mass, then the effective Rydberg in EuTe is $R^* = \hbar^2/2m^*a_B^2 = 0.090$ eV. The very strong localization of the hole in an inner Eu orbital makes negligible its exchange interaction with surrounding lattice spins; hence, the hole does not contribute to the exchange field generating the SP.

The self-energy of the photoexcited electron was found by summing the exchange interaction energy between the photoexcited electron, and all Eu atoms contained the SP sphere, whose radius was taken to be $R_{Pol} = 4a$.[6]

In addition to the well-established input parameter $J_{Xf}S = 0.29$ eV,[6] the MCS required parameters J_1 and J_2, the first and second neighbor exchange interaction constants for EuTe, respectively. A wide range of values for these two parameters is available in the literature. We experimented three different sets of values for J_1 and J_2: by Wachter,[30] Oliveira *et al.*,[31] and Söllinger *et al.*[32]; see Table I.

At each temperature, Monte Carlo iterations were performed until the average self-energy converged. For each temperature, a statistical ensemble of 5000 SPs was generated. The mean Σ in the ensemble determines the energy position of the ZPL, whereas the mean square deviation of Σ gives the FWHM of the ZPL. As an example, Fig. 3 shows histograms for the Σ incidence in the ensemble, for a bin width of 0.5 meV, for $T = 5$, 15, and 30 K. The histograms obey a Gaussian distribution at all temperatures (full lines in Fig. 3).

TABLE I. Input parameters J_1 and J_2 used in the Monte Carlo simulations. The FWHM of the expected PL line at 5 K, the Néel temperature, and the slope of $h\nu_{ZPL}$ at 15 K, obtained from MCS, are shown. The last line shows the corresponding values obtained from the PL spectra.

Reference	J_1 (K)	J_2 (K)	FWHM at 5K (meV)	Néel temperature (K)	$dh\nu_{ZPL}/dT$ at 15 K (meV/K)
Wachter[30]	0.043	−0.150	17	6.9	1.7
Oliveira *et al.*[31]	0.100	−0.215	17	9.6	1.7
Söllinger *et al.*[32]	0.192	−0.313	15	11	0.6
Experimental	⋯	⋯	19	10.5	1.7

Published under an exclusive license by AIP Publishing

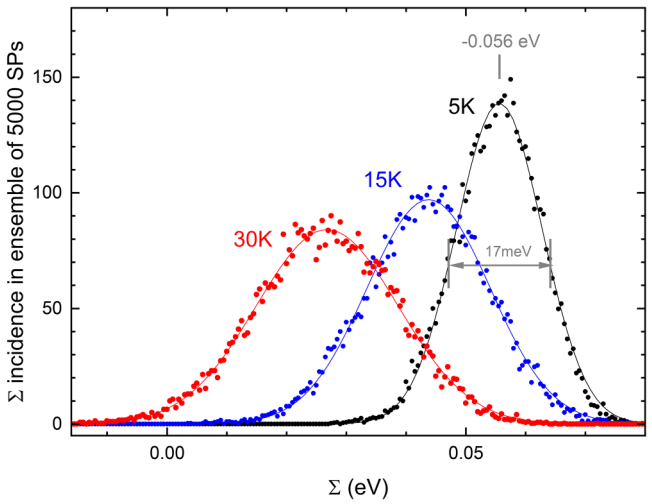

FIG. 3. Histograms for the Σ energy, obtained from MCS, at $T = 5$, 15, and 30 K. The statistical ensemble contained 5000 SPs, and the bin width was set to 0.5 meV.

The experimentally measured temperature dependence of the ZPL maximum, $h\nu_{ZPL}$, was fitted with Eq. (2), whereby $R^* = 0.090$ eV, $E_G = 2.32$ eV,[18] and $\Sigma(T)$ was obtained by our MCS. The best results were obtained using the parameters J_1 and J_2 by Oliveira *et al.* since the same parameters, by Söllinger *et al.* or by Wachter, gave either the wrong slope of $h\nu_{ZPL}$ or the wrong Néel temperature; see Table I. In the fitting, E_{loc} was the only adjustable parameter, giving $E_{loc} = 0.29$ eV; see Fig. 4. The temperature dependence of $h\nu_{ZPL}$ obtained by MCS is in excellent agreement with the experimental data, except for the ordered phase below the Néel temperature, where a small disagreement of a few

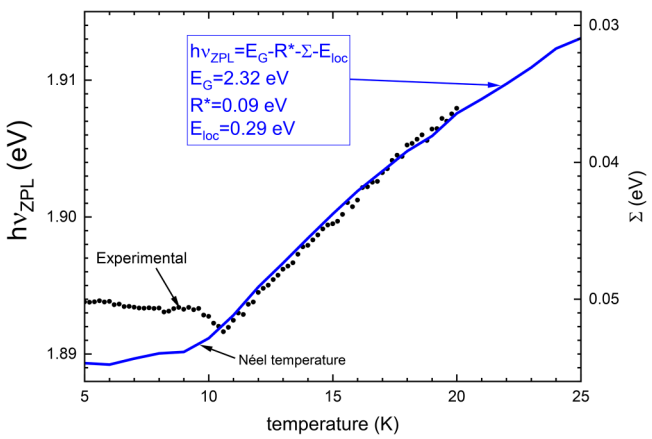

FIG. 4. Photon energy at the peak of the ZPL photoluminescence as a function of temperature (dots). The full line shows the result of the Monte Carlo simulations.

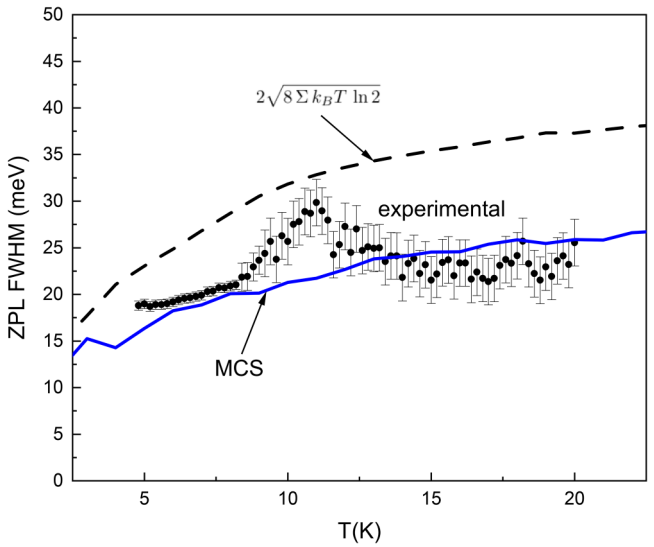

FIG. 5. Temperature dependence of the FWHM of the ZPL photoluminescence. Dots are the experimental values, full line is the result of the MCS, and the dashed line is the result predicted by Dietl and Spalek.[34]

meV is observed, possibly due to the magnetic anisotropy,[33] not included in the MCS.

Furthermore, Fig. 5 shows the temperature dependence of FWHM of the ZPL photoluminescence, predicted by the MCS (full line), as well as the experimentally measured values (dots). The agreement is quite good except that around the Néel temperature, the experimental FWHM shows a mild cusp, probably associated with the anisotropy field acting on the spins, which was not included in the MCS. It is interesting to compare the temperature dependence of the FWHM of the ZPL with the predicted behavior by the thermodynamic model, developed by Dietl and Spalek,[34,35] which yields a simple formula connecting the FWHM of the statistical distribution of the SP self-energy, Σ, to the absolute value of Σ and to the temperature, i.e., $\text{FWHM} = 2\sqrt{8\,\Sigma\,k_B T\,\ln 2}$. Figure 5 shows that the thermodynamic model agrees within 20% with the experimental data.

IV. PL AS A FUNCTION OF EXCITATION POWER AT T = 4.8 K

The localization energy, $E_{loc} = 0.29$ eV, determined in Sec. III indicates that the SPs, associated with the MX_0 band, are bound to defects. In this section, we shall determine the density of these defects by investigating the intensity of the MX_0 photoluminescence as a function of excitation power.

Figure 6(a) shows a stacked plot of the PL spectrum as a function of the excitation power, which was varied over five orders of magnitude, and Fig. 6(b) shows a plot of the integrated intensity vs excitation power. At very low powers, when the MX_0 multiphonon structure is still well resolved, the integrated PL intensity increases sharply. As the excitation power increases, the multiphonon

Published under an exclusive license by AIP Publishing

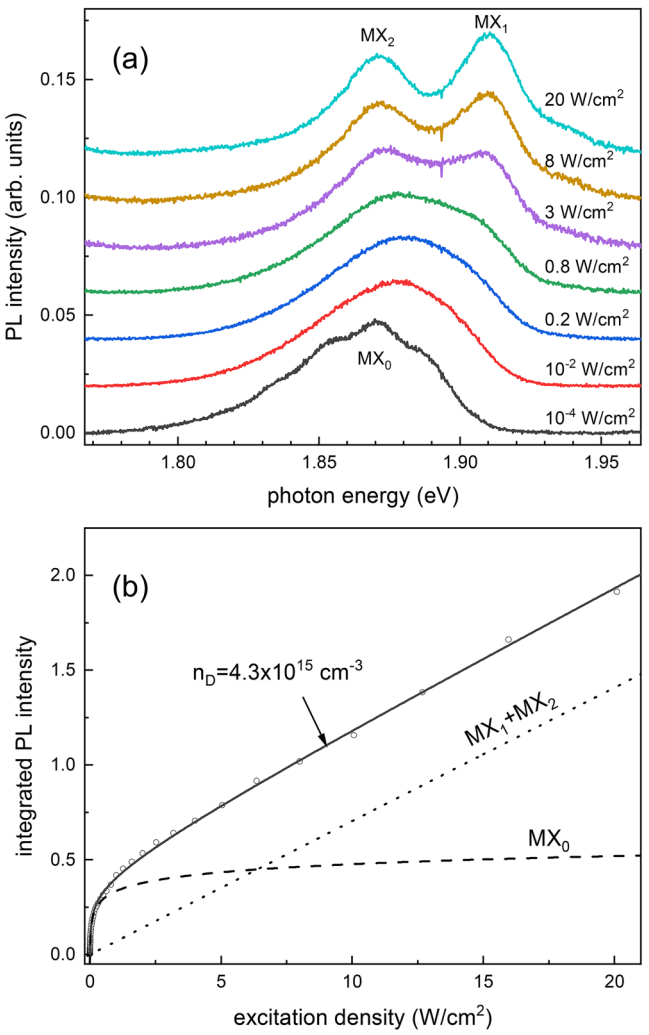

FIG. 6. (a) Stacked plot of the normalized PL spectra as a function of excitation power at $T = 5$ K. (b) Integrated PL intensity as a function of the excitation power density (dots). The full curve is the theoretical fit, which yields the indicated defect density.

structure is washed out, the PL intensity increases more slowly, and two new lines appear, denoted MX_1 and MX_2, as in Ref. 36. In contrast to the MX_0 band, the intensity of the MX_1 and MX_2 bands increases linearly with excitation power.

This behavior suggests that, at all excitation powers, the PL spectrum is a superposition of the MX_0, MX_1 and MX_2 bands, whose relative intensities depend on the excitation power. At very low excitation, the MX_0 band grows very quickly and dominates the PL spectrum. However, when the MX_0 band saturates, MX_1 and MX_2 luminescence takes over progressively and dominates at high excitation powers.

The integrated intensity of the MX_0 band is proportional to the number of excited SPs, n_{Pol}, per unit surface. The very fast saturation of the MX_0 band indicates that the maximum density of SPs that can be excited in EuTe is very limited. This demonstrates that the SPs associated with the MX_0 band are not intrinsic: they are bound to low density impurities or defects. Under these circumstances, as shown in Ref. 37, the steady-state photoinduced density of SPs n_{Pol}, for an excitation power per unit area of the sample surface of p, is given by

$$n_{Pol} \sim \frac{n_D}{\alpha} \times \begin{cases} \frac{p}{p_D} & \text{if } p < p_D, \\ \left(1 + \ln \frac{p}{p_D}\right) & \text{if } p > p_D, \end{cases} \tag{4}$$

where n_D is the density of defects, $p_D = \frac{n_D h\nu}{\chi \alpha \tau_0}$, $h\nu = 2.33$ eV is the excitation photon energy, $\chi = 0.09$ is the excitation quantum efficiency, $\alpha = 10\,\mu m^{-1}$ is the absorption coefficient at the excitation photon energy, and $\tau_0 = 15\,\mu s$ is the SP lifetime.[10]

The integrated PL intensity dependence on excitation power, measured experimentally, was fitted with Eq. (4). To account for the PL associated with MX_1 and MX_2, a linear term was added. The fit depended on only two adjustable parameters: the slope of the added linear term and the density of defects, n_D. An excellent fit was obtained, as shown in Fig. 6. The fit yields the density of defects, $n_D = 4.3 \times 10^{15}$ cm^{-3}. A possible source of defects of such small density could be vacancies due to inexact Eu and Te precursor fluxes during the MBE growth or residual impurities.

Since the MX_0 PL band is produced by photoexcited SPs, it follows that n_D is equal to the maximum density of SPs that can be photoexcited in EuTe. The value $n_D = 4.3 \times 10^{15}$cm^{-3}, deduced from the saturation of the MX_0 PL, is in excellent agreement with $n_D = 4.5 \times 10^{15}$cm^{-3}, found from the saturation of the photoinduced Faraday rotation angle in EuTe.[37] This demonstrates that the MX_0 PL and the photoinduced Faraday rotation are produced by the same SPs.

The saturation of SP density with excitation power, reported in Ref. 37, implies that no SPs associated with PL bands MX_1 or MX_2 could be detected in the photoinduced Faraday rotation experiment. Nevertheless, there is compelling evidence that PL bands MX_1 and MX_2 are also associated with SPs.[36] The nonobservation of Faraday rotation associated with the MX_1 and MX_2 PL bands can be explained by the very short MX_1 and MX_2 PL lifetime of about 1 ns in zero magnetic field.[36] This is four orders of magnitude less than the lifetime of the MX_0 associated SPs, 15 μs.[10] Therefore, for a given excitation power, the steady-state density of MX_1 and MX_2 SPs is going to be four orders of magnitude less than that of MX_0 SPs. Nevertheless, it might be possible to detect MX_1 and MX_2 SPs by photoinduced Faraday rotation measurements, using pulsed light excitation in the sub-picosecond time scale. At ultrashort intervals of time after the arrival of the pump pulse, the population of MX_1 and MX_2 SPs should be much higher than in the steady-state investigated so far, making their detection possible.

Published under an exclusive license by AIP Publishing

V. CONCLUSION

In summary, we showed that photogenerated spin polarons in EuTe are bound to impurities or defects, with a localization energy of 0.29 eV. In the sample studied, the density of defects is only 4.3×10^{15} cm^{-3}, and it is associated with defects due to small non-stoichiometry of the sample or to the presence of residual impurities of a very low concentration. An interesting aspect of the SPs associated with the MX_0 band is their complete immobility due to localization of the hole at an inner atomic orbital of an Eu atom. This implies that bound SPs are not formed due to SP migration toward a defect, which is the usual scenario for bound exciton formation in semiconductors,[28] but rather, SPs are excited at Eu sites where a neighboring defect already exists. This might make it possible to excite resonantly SPs in EuTe, instead of pumping electron–hole pairs through the EuTe gap, as in this work.

It should be stressed that the samples investigated were nominally undoped, and this is why the defect density harboring the SPs is so low. Intentionally increasing the defect density may increase the maximum light-induced magnetization that can be achieved in EuTe.

Our results suggest that a sharp contrast exists between SPs associated with the MX_0 band, on the one hand, and the SPs associated with the MX_1 and MX_2 bands, on the other hand. While the former SPs are associated with defects and have a long lifetime (about 10 μs[10]), the latter appear to be of intrinsic character and have a much shorter lifetime (about 1 ns[36]), which deserves further investigation. Our results also suggest that SPs associated with the MX_1 and MX_2 photoluminescence bands could be detected and characterized by performing time-resolved photoinduced Faraday rotation experiments in the ultrafast time scale.

ACKNOWLEDGMENTS

A. B. H. acknowledges support by CNPq (Grant Nos. 420531/2018-1 and 303757/2018-3) and FAPESP (Grant No. 2020/15570-0).

AUTHOR DECLARATIONS

Conflict of Interest

The authors declare that there is no conflict of interest.

DATA AVAILABILITY

The data that support the findings of this study are available within the article.

REFERENCES

[1]P. G. de Gennes, Phys. Rev. **118**, 141 (1960).
[2]T. Kasuya, A. Yanase, and T. Takeda, Solid State Commun. **8**, 1543 (1970).
[3]E. L. Nagaev, Phys. Status Solidi B **145**, 11 (1988).
[4]A. Mauger and D. L. Mills, Phys. Rev. Lett. **53**, 1594 (1984).
[5]A. Mauger and D. L. Mills, Phys. Rev. B **31**, 8024 (1985).
[6]A. B. Henriques, F. C. D. Moraes, G. D. Galgano, A. J. Meaney, P. C. M. Christianen, J. C. Maan, E. Abramof, and P. H. O. Rappl, Phys. Rev. B **90**, 369 (2014).
[7]J. Kossut and J. A. Gaj, *Introduction to the Physics of Diluted Magnetic Semiconductors*, Springer Series in Materials Science Vol. 144 (Springer, 2010).
[8]V. G. Storchak, O. E. Parfenov, J. H. Brewer, P. L. Russo, S. L. Stubbs, R. L. Lichti, D. G. Eshchenko, E. Morenzoni, T. G. Aminov, V. P. Zlomanov, A. A. Vinokurov, R. L. Kallaher, and S. von Molnár, Phys. Rev. B **80**, 235203 (2009).
[9]A. B. Henriques, G. D. Galgano, E. Abramof, B. Diaz, and P. H. O. Rappl, Appl. Phys. Lett. **99**, 091906 (2011).
[10]A. B. Henriques, G. D. Galgano, P. H. O. Rappl, and E. Abramof, Phys. Rev. B **93**, 570 (2016).
[11]A. B. Henriques, X. Gratens, P. A. Usachev, V. A. Chitta, and G. Springholz, Phys. Rev. Lett. **120**, 217203 (2018).
[12]X. Gratens, Y. Ou, J. S. Moodera, P. H. O. Rappl, and A. B. Henriques, Appl. Phys. Lett. **116**, 152402 (2020).
[13]S. C. P. van Kooten, X. Gratens, and A. B. Henriques, Phys. Rev. B **103**, 035202 (2021).
[14]E. Granado, E. Abramof, P. H. O. Rappl, V. A. Chitta, and A. B. Henriques, Phys. Rev. B **78**, 175 (2008).
[15]A. B. Henriques, G. D. Galgano, B. L. Díaz, P. H. O. Rappl, and E. Abramof, J. Phys.: Condens. Matter **19**, 406234 (2007).
[16]A. Mauger and C. Godart, Phys. Rep. **141**, 51 (1986).
[17]A. B. Henriques, A. Wierts, M. A. Manfrini, G. Springholz, P. H. O. Rappl, E. Abramof, and A. Y. Ueta, Phys. Rev. B **72**, 155337 (2005).
[18]A. B. Henriques, M. A. Manfrini, P. H. O. Rappl, and E. Abramof, Phys. Rev. B **77**, 035204 (2008).
[19]A. B. Henriques and P. A. Usachev, Phys. Rev. B **96**, 679 (2017).
[20]S. C. P. van Kooten, P. A. Usachev, X. Gratens, A. R. Naupa, V. A. Chitta, G. Springholz, and A. B. Henriques, J. Appl. Phys. **126**, 095701 (2019).
[21]B. Kaminski *et al.*, Phys. Rev. Lett. **103**, 057203 (2009).
[22]A. B. Henriques, E. Abramof, and P. H. O. Rappl, Phys. Rev. B **80**, 301 (2009).
[23]M. Lafrentz, D. Brunne, B. Kaminski, V. V. Pavlov, A. B. Henriques, R. V. Pisarev, D. R. Yakovlev, G. Springholz, G. Bauer, E. Abramof, P. H. O. Rappl, and M. Bayer, Phys. Rev. B **82**, 235206 (2010).
[24]G. D. Holah, J. S. Webb, R. B. Dennis, and C. R. Pidgeon, Solid State Commun. **13**, 209 (1973).
[25]A. B. Henriques and J. P. von der Weid, Solid State Commun. **56**, 571 (1985).
[26]H. B. Bebb and E. W. Williams, in *Semiconductors and Semimetals* (Academic Press, London, 1972), Vol. 8, p. 299.
[27]P. J. Dean and D. C. Herbert, in *Topics in Current Physics* (Springer-Verlag, Berlin, 1979), Vol. 14, p. 55.
[28]B. K. Meir, in *Zinc Oxide: From fundamental properties towards novel applications*, Springer Series in Materials Science (Springer-Verlag, Berlin, 2010), Vol. 120, p. 169.
[29]J. Vinins and P. Wachter, Phys. Rev. B **12**, 3829 (1975).
[30]P. Wachter, CRC Crit. Rev. Solid State Sci. **3**, 189 (1972).
[31]N. F. Oliveira, S. Foner, and Y. Shapira, Phys. Rev. B **5**, 2634 (1972).
[32]W. Söllinger, W. Heiss, R. T. Lechner, K. Rumpf, P. Granitzer, H. Krenn, and G. Springholz, Phys. Rev. B **81**, 155213 (2010).
[33]J. W. Battles and G. E. Everett, Phys. Rev. B **1**, 3021 (1970).
[34]T. Dietl and J. Spalek, Phys. Rev. Lett. **48**, 355 (1982).
[35]T. Dietl, J. Magn. Magn. Mater. **38**, 34 (441983).
[36]W. Heiss, R. Kirchschlager, G. Springholz, Z. Chen, M. Debnath, and Y. Oka, Phys. Rev. B **70**, 484 (2004).
[37]A. B. Henriques, A. R. Naupa, P. A. Usachev, V. V. Pavlov, P. H. O. Rappl, and E. Abramof, Phys. Rev. B **95**, 045205 (2017).

Published under an exclusive license by AIP Publishing